第 31 卷第 6 期
2015 年 6 月

无 机 化 学 学 报
CHINESE JOURNAL OF INORGANIC CHEMISTRY

Vol.31 No.6
1231-1238

以 T 型三羧酸配体构筑的具有 2D→3D 穿插结构的金属有机框架的合成、结构及性质

段艳林　马然然　曹婷婷　刘　婷　李成娟*　王素娜*

(山东省化学储能与储氢重点实验室,聊城大学化学化工学院,聊城　252000)

摘要：采用溶剂热合成法,利用 T 型三羧酸配体 3,4′,5-联苯三羧酸(H_3BPT=biphenyl-3,4′,5-tricarboxylic acid)制备并表征了 2 个 2D→3D 穿插结构的金属有机框架结构,$\{[Ni_3(BPT)_2(bpe)_2(H_2O)_6]\cdot 2DMF\cdot 7H_2O\}_n$ (**1**)和$\{[Ni_3(BPT)_2(bpea)_2(H_2O)_6]\cdot 2DMF\cdot 5H_2O\}_n$ (**2**) (bpe=1,2-bis(4-pyridyl)ethylene,bpea=1,2-bis(4-pyridyl)ethane,DMF=*N*,*N*-dimethylformamide)。在这 2 个化合物中,BPT 配体和含氮配体 bpe 或 bpea 共同连接相邻的 Ni(Ⅱ)中心,形成(3,4)-连接的$(6^3)(6^5.8)$二维双层结构。相邻双层结构间相互穿插,形成具有聚轮烷结构的 2D→3D 互锁结构。气体吸附性质表明,化合物 **1** 对 CO_2 和 N_2 具有一定的吸附能力。

关键词：金属有机框架；穿插结构；3,4′,5-联苯三羧酸

中图分类号：O614.81+3　　**文献标识码**：A　　**文章编号**：1001-4861(2015)06-1231-08

DOI:10.11862/CJIC.2015.132

Two Unusual 2D→3D Entanglement Networks Self-Assembled from a T-shaped Tricarboxylate Ligand: Syntheses, Structures and Properties

DUAN Yan-Lin　MA Ran-Ran　CAO Ting-Ting　LIU Ting　LI Cheng-Juan*　WANG Su-Na*

(*Shandong Provincial Key Laboratory of Chemical Energy Storage and Novel Cell Technology, School of Chemistry and Chemical Engineering, Liaocheng University, Liaocheng, Shandong* 252000, *China*)

Abstract: Two Ni(Ⅱ)-organic frameworks, namely, $\{[Ni_3(BPT)_2(bpe)_2(H_2O)_6]\cdot 2DMF\cdot 7H_2O\}_n$ (**1**) and $\{[Ni_3(BPT)_2(bpea)_2(H_2O)_6]\cdot 2DMF\cdot 5H_2O\}_n$ (**2**) (H_3BPT = biphenyl-3,4′,5-tricarboxylic acid, bpe = 1,2-bis(4-pyridyl)ethylene, bpea=1,2-bis(4-pyridyl)ethane, DMF=*N*,*N*-dimethylformamide), were solvothermally synthesized and characterized. In the two isostructural complexes, BPT ligand and N-containing ligand bpea or bpe connect adjacent Ni centers to form a bilayer structure. The whole topology could be represented as (3,4)-connected $(6^3)(6^5.8)$ with the tricarboxylate ligands and Ni atoms as 3-connected T-shaped and 4-connected tetrahedral nodes, respectively. Each bilayer polycatenates two other identical bilayers, giving rise to a 2D→3D polycatenating network with polyrotaxane moieties. Gas adsorptive measurements indicated compound **1** exhibited adsorption of CO_2 and N_2. CCDC: 1048385, **1**; 1048386, **2**.

Key words: metal-organic framework; polycatenating; biphenyl-3,4′,5-tricarboxylic acid

Construction of coordination polymers (CPs) or metal-organic frameworks (MOFs) has attracted more and more attention in recent years not only for potential applications but also for fascinating architectures and topologies[1-6]. Entanglement systems, such as polycatenation, polythreading, polyknotting, as

收稿日期:2015-02-10。收修改稿日期:2015-03-26。

国家自然科学基金(No.20801025),山东省自然科学基金(No.ZR2012BQ023),山东省高等学校科技计划项目(No.J14LC10)资助。

*通讯联系人。E-mail:wangsuna@lcu.edu.cn,lichengjuan@lcu.edu.cn;会员登记号:S06N2135M1004。

well as Borromean links, are of special interest [7-9]. Polycatenation indicates that the lower dimensional polymeric structures can generate a structure of overall higher dimensionality through entanglement, such as 1D→2D[10-12] and 2D→3D[13-16]. Each individual motif is catenated only with the surrounding ones and not with all the others. Polythreaded structures, however, are characterized by the presence of closed loops and elements that can thread through the loops, which can be considered as extended periodic analogues of molecular rotaxanes and pseudorotaxanes. To our knowledge, most encountered cases containing both polyrotaxane and polycatenane motifs display a parallel 2D→2D interlocking mode[17-21]; only a few examples display an inclined 2D→3D interlocking mode[22-24] since the first 2D→3D parallel interpenetration was reported in 1997[25]. Most of these frameworks are constructed from simple 2D (4,4) or (6,3) layers with side arms.

Recently, we have reported a series of entangled metal-organic frameworks with interpenetrating/self-penetrating properties[26-29]. Herein, we report two isostructural Ni coordination complexes, $\{[Ni_3(BPT)_2(bpe)_2(H_2O)_6]\cdot 2DMF\cdot 7H_2O\}_n$ (**1**) and $\{[Ni_3(BPT)_2(bpea)_2(H_2O)_6]\cdot 2DMF\cdot 5H_2O\}_n$ (**2**) (H_3BPT=biphenyl-3,4′,5-tricarboxylic acid, bpe=1,2-bis(4-pyridyl)ethylene, bpea=1,2-bis(4-pyridyl)ethane, DMF=*N*,*N*-dimethylformamide). Connection of Ni centers with BPT and N-containing colig-ands led to a (3,4)-connected $(6^3)(6^5.8)$ bilayer struc-ture with the tricarboxylate ligands and Ni atoms as 3-connected T-shaped and 4-connected tetrahedral nodes, respectively. Each bilayer polycatenates other two identical bilayers, giving rise to a porous 2D→3D polycatenating network with polyrotaxane moieties.

1 Experimental

1.1 Reagents and physical measurements

H_3BPT was purchased from Jinan Henghua Sci. & Technol. Co. Ltd. bpe and bpea were purchased from Sigma-Aldrich. Other reagents were used as purchased without further purification. The elemental analysis was carried out with a Perkin-Elmer 240C elemental analyzer. The FT-IR spectra were recorded from KBr pellets in the range of 4 000~400 cm^{-1} on a VECTOR 22 spectrometer. Powder X-ray diffraction (PXRD) data were collected over the 2θ range of 5°~50° on a Philips X′pert diffractometer using Cu $K\alpha$ radiation (λ=0.154 18 nm) at room temperature. Thermal analyses were performed on a TGA V5.1A Dupont 2100 instrument from room temperature to 700 ℃ with a heating rate of 10 ℃·min^{-1} under flowing nitrogen. Gas sorption isotherms were measured using a Quantam-IQ-c analyzer. The N_2 and CO_2 adsorption isotherms for desolvated **1** were collected in a pressure range from 10 to 1.0×10^5 Pa. The cryogenic temperatures of 77 K required for N_2 sorption measurements were controlled by liquid nitrogen, and the 273 K required for CO_2 was controlled using an ice-water bath. The initial out-gassing process for the sample was carried out under a high vacuum (less than 10^{-4} Pa) at 80℃ for 10 h.

1.2 Synthesis of $\{[Ni_3(BPT)_2(bpe)_2(H_2O)_6]\cdot 2DMF\cdot 7H_2O\}_n$ (1) and $\{[Ni_3(BPT)_2(bpea)_2(H_2O)_6]\cdot 2DMF\cdot 5H_2O\}_n$ (2)

Both complexes were solvothermally synthesized. In a general procedure, $Ni(NO_3)_2\cdot 6H_2O$ (0.029 g, 0.1 mmol), H_3BPT (0.029 g, 0.1 mmol), bpe or bpea (0.018 g, 0.1 mmol) were added to a mixed solvent system of DMF (3 mL), CH_3OH (9 mL) and H_2O (2 mL). The mixture was placed in a Teflon reactor and heated at 373 K for 48 h. After cooling to room temperature, blue crystals of compounds **1** or **2** were obtained (36% and 39% yields based on $Ni(NO_3)_2\cdot 6H_2O$, respectively). For **1**: Elemental analysis Calcd. for $C_{60}H_{74}N_6O_{27}Ni_3$(%): C 48.45, H 5.01, N 5.65; Found: C 49.20, H 4.97, N 5.50. FT-IR (KBr pellet, cm^{-1}): 3 446s, 1 633s, 1 585m, 1 386m, 1 281w, 1 078m, 772m. For **2**: Elemental analysis Calcd. for $C_{60}H_{74}N_6O_{25}Ni_3$ (%): C 49.45, H 5.12, N 5.77; Found: 49.83, H 5.03, N 5.62. FT-IR (KBr pellet, cm^{-1}): 3 421br, s, 1 669m, 1 615m, 1 533s, 1 440m, 1 394s, 1 069w, 1 025w, 833w, 771m, 552w.

1.3 X-ray single crystal structures collection and refinement

Suitable single crystal of compound **1** was measured using Agilent at 135 K. Crystal of compound

2 was selected for indexing and intensity data were measured using a Siemens Smart CCD diffractometer with graphite-monochromated Mo $K\alpha$ radiation (λ = 0.071 073 nm) at 298 K. The structures were solved with direct methods and refined by full-matrix least-squares methods using the SHELXS-97 and SHELXL-97 programs, respectively[30-31]. The coordinates of the non-hydrogen atoms were refined anisotropically. Both structures were examined using the ADDSYM subroutine of PLATON to ensure that no additional symmetry could be applied to the models. Topological analysis of coordination networks in both compounds was performed with the program package TOPOS[32].

In compounds **1** and **2**, several disordered atoms were observed. In compound **1**, C atoms (C21/C21′ and C22/C22′) of the ethylene groups in bpe were disordered over two positions, respectively, and were refined with a site occupation factor of 2.14∶1. The solvent DMF molecules, aqua molecules (O13/O13′) are refined with a site occupation factor of 1∶1. The disordered solvent aqua molecules (O14/O14′) were refined with a site occupation factor of 4∶1. The aqua molecules (O15/O17) were refined with a site occupation factor of 1∶1. In compound **2**, the O2 atoms of the carboxylate group were distributed over two positions, and they were all refined with a site occupation factor of 1.74∶1. The coordinated aqua molecules O8 and O9 were all disordered over two positions, respectively. O8/O8′ and O9/O9′ were refined with a site occupation factor of 1.15∶1. C atoms (C23/C23′, C24/C24′, C26/C26′ and C27/C27′) on the pyridyl ring of the bpea ligand were refined with a site occupation factor of 1.08∶1. The solvent DMF and aqua molecules were all half occupied.

CCDC: 1048385, **1**; 1048386, **2**.

2 Results and discussion

2.1 Description of the structures

Solvothermal treatment of a mixture of $Ni(NO_3)_2\cdot 6H_2O$, BPT and bpe or bpea in DMF/CH_3OH/H_2O at 373 K for 48 h gave rise to green crystals of compounds **1** and **2**, respectively. Single crystal X-ray diffraction

Table 1　Crystal data and structure refinement information for compounds 1 and 2

Compound	**1**	**2**
Formula	$C_{60}H_{74}N_6Ni_3O_{27}$	$C_{60}H_{74}N_6Ni_3O_{25}$
Formula weight	1 487.38	1 455.38
Crystal system	Triclinic	Triclinic
Space group	$P\bar{1}$	$P\bar{1}$
a / nm	1.011 90(7)	1.016 60(11)
b / nm	1.350 70(14)	1.342 19(15)
c / nm	1.385 86(17)	1.401 01(17)
α / (°)	66.365(11)	113.148(2)
β / (°)	87.230(7)	91.001 0(10)
γ / (°)	76.928(7)	99.749 0(10)
V / nm^3	1.688 4(3)	1.724 9(3)
Z	1	1
D_c / (g·cm^{-3})	1.463	1.401
μ / mm^{-1}	1.716	0.891
θ range for data collection	3.67~66.05	2.47~25.02
Limiting indices	$-11 \leqslant h \leqslant 9$, $-15 \leqslant k \leqslant 16$, $-14 \leqslant l \leqslant 16$	$-9 \leqslant h \leqslant 12$, $-15 \leqslant k \leqslant 15$, $-14 \leqslant l \leqslant 16$
Reflections collected / unique (R_{int})	10 076 / 5 812(0.051 5)	8 675 / 5 983(0.030 9)
Final R indices ($I \geqslant 2\sigma(I)$) R_1, wR_2[a]	0.078 5, 0.173 4	0.059 8, 0.165 3
R indices (all data) R_1, wR_2[a]	0.105 1, 0.187 6	0.084 8, 0.191 5
Goodness-of-fit on F^2	1.069	1.045

[a] $R_1=\sum||F_o|-|F_c||/|F_o|$; $wR_2=[\sum w(\sum F_o^2-F_c^2)^2/\sum w(F_o^2)^2]^{1/2}$

Table 2 Selected bond lengths (nm) and angles (°) of compounds 1 and 2

1					
Ni(1)-O(1)	0.215 2(4)	Ni(1)-O(4)^{iii}	0.202 4(4)	Ni(2)-O(8)^{i}	0.206 8(4)
Ni(1)-N(1)	0.207 8(4)	Ni(1)-O(7)	0.207 8(4)	Ni(2)-O(9)^{i}	0.206 1(4)
Ni(1)-N(2)^{ii}	0.208 3(4)	Ni(2)-O(5)	0.204 2(4)	Ni(2)-O(9)	0.206 1(4)
Ni(1)-O(2)	0.210 8(3)	Ni(2)-O(5)^{i}	0.204 2(4)	Ni(2)-O(8)	0.206 8(4)
N(1)-Ni(1)-N(2)^{ii}	176.9(2)	O(5)-Ni(2)-O(5)^{i}	180.00(15)	O(4)^{iii}-Ni(1)-N(2)^{ii}	92.76(17)
N(2)^{iii}-Ni(1)-O(2)	90.28(16)	O(9)-Ni(2)-O(9)^{i}	180.00(15)	O(4)^{iii}-Ni(1)-O(2)	160.02(14)
N(1)-Ni(1)-O(1)	84.62(16)	O(9)-Ni(2)-O(8)	89.42(16)	N(1)-Ni(1)-O(2)	87.60(16)
N(2)-Ni(1)-O(1)	96.35(16)	O(7)-Ni(1)-N(2)^{ii}	87.36(16)	O(7)-Ni(1)-O(2)	104.19(14)
O(2)-Ni(1)-O(1)	61.98(13)	O(4)^{iii}-Ni(1)-N(1)	89.98(18)	O(5)-Ni(2)-O(8)^{i}	89.82(16)
O(7)-Ni(1)-O(1)	165.57(14)	O(4)^{iii}-Ni(1)-O(7)	95.68(15)		
O(4)^{iii}-Ni(1)-O(1)	98.06(14)	N(1)-Ni(1)-O(7)	90.99(17)		
2					
Ni(1)-O(1)	0.202 5(3)	Ni(1)-O(3)^{i}	0.210 6(3)	Ni(2)-O(8)	0.208 8(8)
Ni(1)-N(1)	0.208 4(4)	Ni(1)-O(4)^{i}	0.217 4(3)	Ni(2)-O(6)^{iii}	0.203 6(3)
Ni(1)-N(2)^{ii}	0.209 2(4)	Ni(2)-O(6)	0.203 6(3)	Ni(2)-O(8)^{iii}	0.208 8(8)
Ni(1)-O(7)	0.209 5(3)	Ni(2)-O(9)	0.205 8(7)	Ni(2)-O(9)^{iii}	0.205 8(7)
N(1)-Ni(1)-O(4)^{i}	86.07(15)	N(1)-Ni(1)-N(2)^{ii}	177.43(17)	O(1)-Ni(1)-O(7)	94.81(14)
O(1)-Ni(1)-N(1)	89.35(16)	O(6)-Ni(2)-O(9)	94.2(2)	O(7)-Ni(1)-O(3)^{i}	103.81(13)
N(2)^{ii}-Ni(1)-O(3)^{i}	90.61(15)	O(9)-Ni(2)-O(8)	90.8(3)	O(1)-Ni(1)-O(4)^{i}	99.57(13)
N(1)-Ni(1)-O(3)^{i}	87.82(15)	N(2)^{ii}-Ni(1)-O(4)^{i}	94.98(15)	O(7)-Ni(1)-O(4)^{i}	164.94(14)
O(1)-Ni(1)-O(3)^{i}	161.14(13)	N(2)^{ii}-Ni(1)-O(7)	88.75(16)	O(3)^{i}-Ni(1)-O(4)^{i}	61.64(12)
O(1)-Ni(1)-N(2)^{ii}	92.78(15)	N(1)-Ni(1)-O(7)	89.65(16)	O(6)-Ni(2)-O(8)	90.5(2)

Symmetry transformations used to generate equivalent atoms: ^{i} 1−*x*, 1−*y*, 2−*z*; ^{ii} *x*, 1+*y*, *z*; ^{iii} 1+*x*, *y*, *z* for **1**; ^{i} 1+*x*, *y*, *z*; ^{ii} *x*, 1+*y*, *z*; ^{iii} −*x*, 1−*y*, −*z* for **2**

studies indicated that these two compounds are isostructural and only compound **1** is described representatively. Compound **1** crystallizes in the triclinic crystal system and space group $P\bar{1}$. As shown in Fig.1, the asymmetric unit is composed of two crystallographically independent Ni centers, one BPT

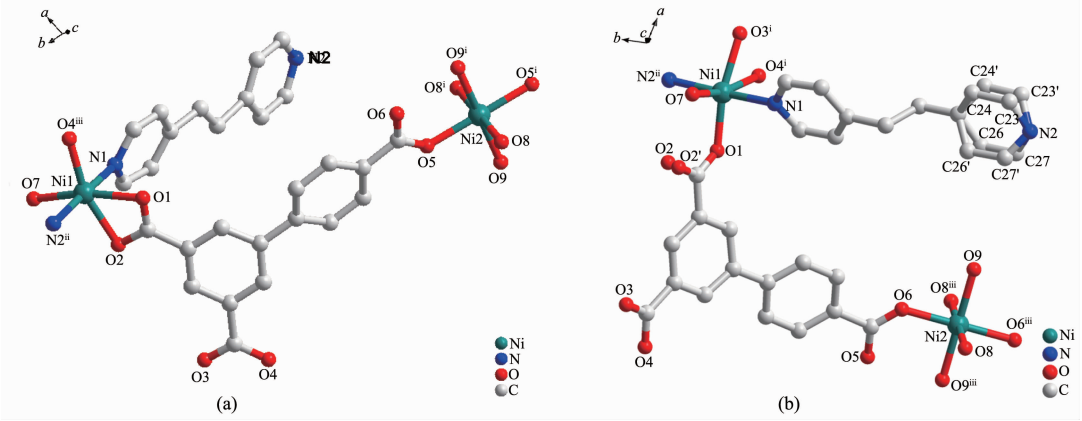

Hydrogen atoms have been omitted for clarity; Symmetry codes: for **1**: ^{i} 1−*x*, 1−*y*, 2−*z*; ^{ii} *x*, 1+*y*, *z*; ^{iii} 1+*x*, *y*, *z*; for **2**: ^{i} 1+*x*, *y*, *z*; ^{ii} *x*, 1+*y*, *z*; ^{iii} −*x*, 1−*y*, −*z*

Fig.1 Local coordination environment of the Ni(Ⅱ) centers in compounds **1** (a) and **2** (b), respectively

ligand, one bpe ligand and two aqua molecules. Both Ni centers adopt six-coordinated octahedral coordination geometry. The coordination spheres are different, however. For Ni1, the equatorial plane of the octahedron is composed of two chelating carboxylate oxygen atoms (O1 and O2), one monodentate carboxylate oxygen atom ($O4^{ii}$) (Symmetry code: ^{ii} x, $1+y$, z) from two different BPT ligands as well as one aqua oxygen atom (O7). Two nitrogen atoms (N1 and $N2^{ii}$) from two bpe ligands occupy the axial positions. Ni2 at the site with centrosymmetry, however, is surrounded by four aqua oxygen atoms (O8, O9, $O8^{i}$ and $O9^{i}$) and two monodentate carboxylate oxygen atoms (O5 and $O5^{i}$) (Symmetry code: ^{i} $1-x$, $1-y$, $2-z$) of two different BPT ligands. The Ni-O and Ni-N distances are in the range of 0.202 0(4)~0.216 0(5) nm, respectively.

Each BPT ligand adopts μ^3-η^1:η^1:η^2 mode, connecting two Ni1 atoms and one Ni2 atom, forming a ladder structure along the a axis with Ni1⋯$Ni1^{i}$ and Ni1⋯$Ni1^{ii}$ (Symmetry codes: ^{i} $1-x$, $1-y$, $2-z$; ^{ii} x, $1+y$, z;) separations of 1.014 5(1) and 2.351 0(2) nm across the ladder (Fig.2a). These ladders are pillared by bpe bridges to give a 2D bilayer structure in parallel with the ac plane (Fig.2b). Topologically, BPT ligand and Ni1 centers could be considered as 3-connected T-shaped and 4-connected distorted tetrahedral nodes, respectively. The Schläfli symbol of the whole bilayer is represented as (3,4)-connected $(6^3)(6^5.8)$ with long symbol of $(6.6^2.6)(6.6.6.6.6)$[32] (Fig.3). To the best of our knowledge, examples of molecular bilayers constructed by 'T-shaped' modules are still rare so far. The T-shaped modules are generally metal centers with T-shaped coordination configuration through three 'spacer' ligands[33-36]. To get T-shaped modules by 'T-shaped' ligands could be considered as another strategy. Recently, a coordination polymer assembled from the BPT ligand, namely, $\{[Cd_3(BPT)_2(H_2O)_9]\cdot(H_2O)_5\}_n$[37], has been reported. The BPT ligands bridge Cd centers to form a typical T-shaped molecular bilayer motif subunit, which is inclined to form multi-dimensional structures. The difference lies in the fact that the individual bilayer is of an $(8^2.10)$ topology with the ligands as 3-connected T-shaped nodes.

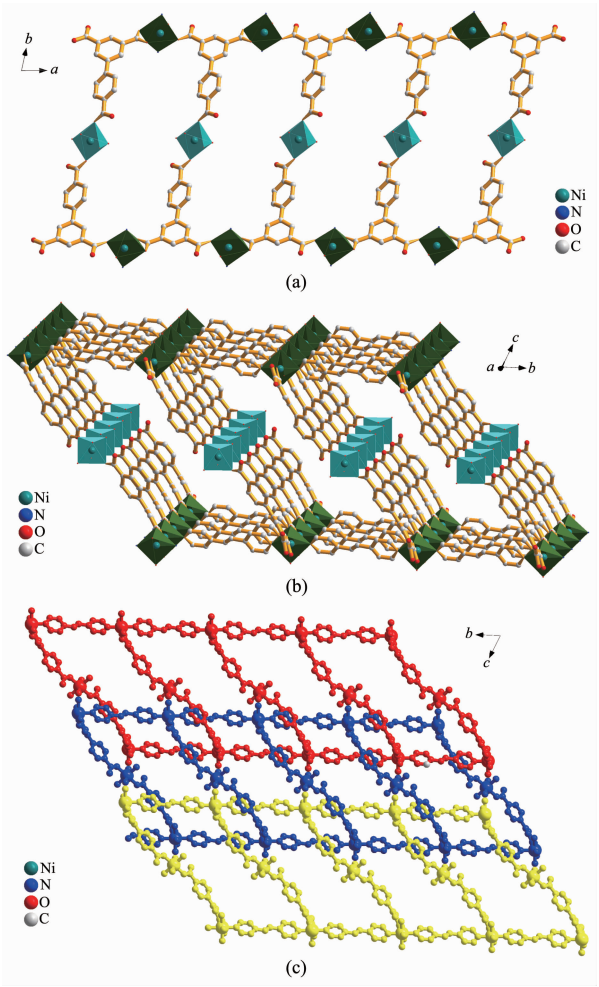

Fig.2 (a) Perspective views of the 1D ladders constructed by BPT and Ni centers along the *a* axis; (b) Perspective view of the 2D bilayer structure of compound **1** in parallel with the *bc* plane; (c) Perspective view of the parallel polycatenation of three different bilayers

The most fascinating and peculiar structural feature of compounds **1** and **2** is that these two coordination polymers show both polyrotaxane and polycatenane character. Through the special connection of metals and ligands, 1D nanotubes are observed along both the *a* and *b* axis within the bilayer. The dimensions of these tubes are 1.350 7(2) nm×2.349 7(4) nm (1.342 19(18) nm×2.345 43(16) nm for compound **1** and 1.011 90(14) nm×2.349 7(4) nm (1.016 60(13) nm×2.34543(16) nm for compound **2** based on the separation of opposite metal centers, respectively. As expected, the large dimension allows them to interpenetrate in an extensive and unusual fashion.

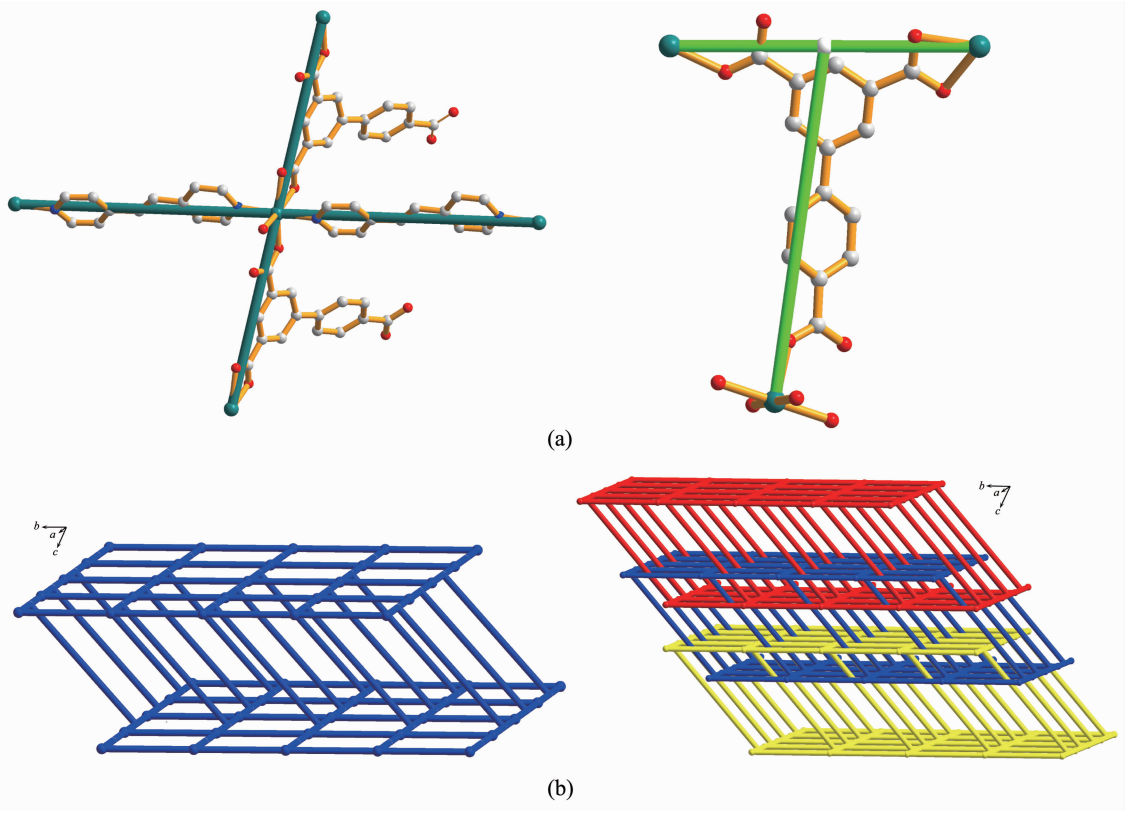

Fig.3 (a) View of the 3- and 4-connected nodes based on BPT and Ni1 centers; (b) Topological view of the 2D bilayer and 2D→3D interpenetrating networks, respectively

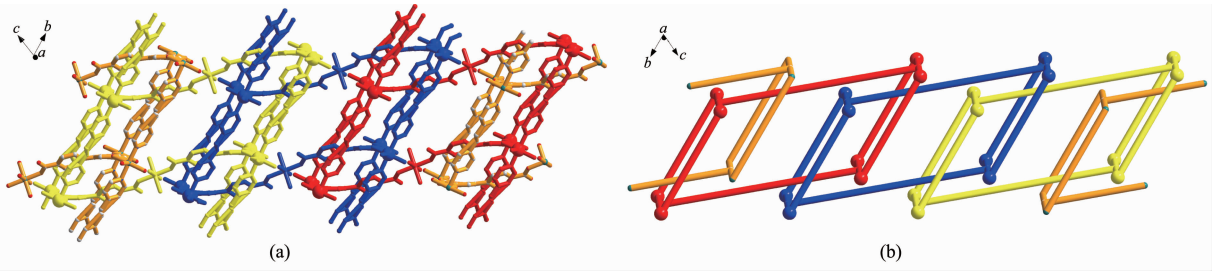

Fig.4 Perspective (a) and schematic (b) views of polycatenation and polyrotaxane motifs within compound **1**

Firstly, each bilayer is aligned parallel to the *c* axis and interlocked in a parallel fashion with two nearest neighboring ones to give rise to a 3D polycatenated structure. Secondly, the bpe-Ni2-bpe part in one bilayer acts as a rod and threads into the $[Ni_2(BPT)_2(bpe)_2]$ or $[Ni_2(BPT)_2(bpea)_2]$ loop from the other two bilayers (Fig.4). As a consequence, these two compounds represent 2D→3D examples having both polycatenane and polyrotaxane characteristics. Due to different N-containing ligands in two complexes, the pillared bpe-Ni2-bpe or bpea-Ni2-bpea parts within the bilayer form different angles (59.861(7)° for **1**; 49.406(4)° for **2**) with respect to the single layer, respectively (Fig.5).

Although such complicated interpenetration has occurred, 1D channels extend along the *a* axis. Calcu-

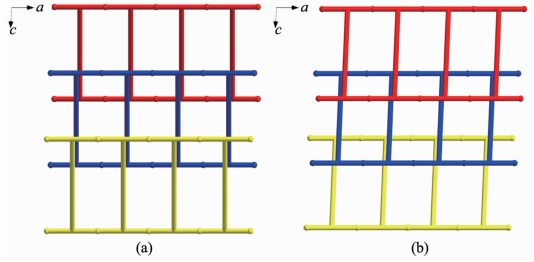

Fig.5 Topological view of the 3-fold interpenetrating motifs of compounds **1** (a) and **2** (b) along the *b* axis, showing the different angles of the T-shaped nodes

lations using PLATON reveal that the dimensions of these channels occupy 29.7% and 26.8% of the whole unit cell[38].

2.2 Powder XRD and TGA

Powder XRD measurements were employed to reveal further structural information. Diffraction patterns of compounds **1** and **2** were displayed in Fig. 6. Almost all peaks actually measured were well fit to those in the simulated curves, indicating the purity of both compounds. Thermogravimetric analysis (TGA) was performed on both compounds to investigate their thermal stability (Fig.7). These two compounds exhibited similar thermal stability, as indicated by well coincidence of the two weight-loss curves. The TG curves of these compounds displayed a steady weight loss from room temperature to 120 ℃ (Weight loss: 18.0% for **1** and 17.6% for **2**), corresponding to the loss of free DMF and H_2O molecules (Calcd. 18.3% for **1** and 17.2% for **2**). Sudden weight loss occurred at 360 and 370 ℃ for **1** and **2**, respectively, accompanied by rapid collapse of the frameworks.

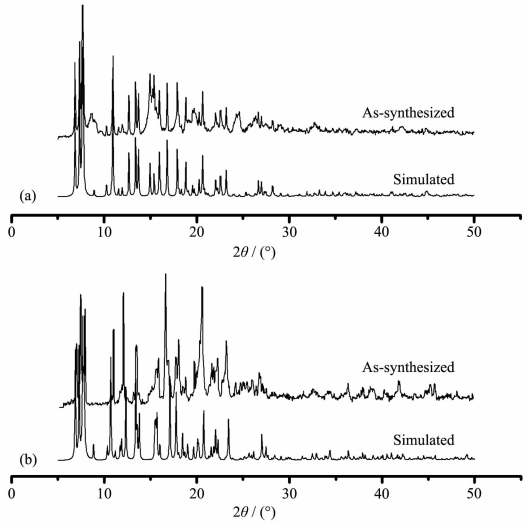

Fig.6　Powder XRD patterns of compounds **1** (a) and **2** (b)

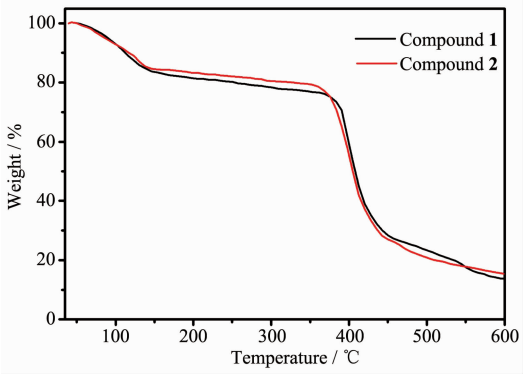

Fig.7　TG curves of compounds **1** and **2**

2.3 Gas absorption properties

In order to investigate the porous properties of the structures, gas sorption measurements were performed. Considering the isostructural structures, only compound 1 was selected representatively. Fresh samples of compound 1 were firstly solvent exchanged with CH_2Cl_2 and then outgassed at 80 ℃ for 10 hours under vacuum. Interestingly, the activated sample of compound 1 hardly adsorbs N_2 gas (3.7 $cm^3 \cdot g^{-1}$ before 9.31×10^4 Pa and 20.6 $cm^3 \cdot g^{-1}$ at 1.0×10^5 Pa) at 77 K but exhibits adsorption for CO_2 up to (29.3 $cm^3 \cdot g^{-1}$) at 273 K and 1.0×10^5 Pa (Fig.8). This selective adsorption behavior has also been found in other reported coordination polymers and could also be attributed to the small apertures of the channels that prevent the entrance of N_2 (Kinetic diameter: 0.364 nm) but allow the diffusion of CO_2 (Kinetic diameter: 0.33 nm) into the channels[39-42]. The gas uptakes are not as high as the pore volume based upon the crystal structure, which may be derived from the partly collapse or shrink of the framework of compound **1** after removal of the solvent molecules.

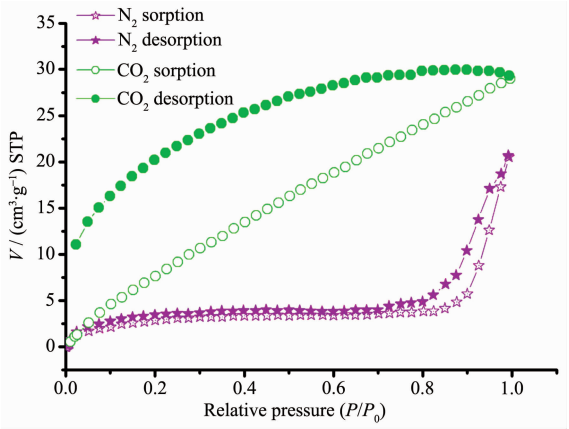

Sorption and desorption data are show as filled and open symbols, respectively

Fig.8　Gas sorption isotherms of the activated compound 1

3 Conclusions

In summary, we have prepared and reported two isostructural 2D →3D polycatenating networks with polyrotaxane moieties. The 2D net could be represented as (3,4)-connected $(6^3)(6^5.8)$ with the tricarboxylate

ligands and Ni atoms as 3-connected T-shaped and 4-connected tetrahedral nodes, respectively. Gas adsorptive measurements indicated compound **1** exhibited adsorption for CO_2 and N_2.

Acknowledgements: We are thankful to the National Natural Science Foundation of China (No.20801025), the Natural Science Foundation of Shandong Province (No. ZR2012BQ023), and the University Scientific Research Development Plan of the Education Department of Shandong Province (No.J14LC10).

References:

[1] Li M, Li D, Yaghi O M, et al. *Chem. Rev.*, **2014**,**114**:1343-1370

[2] Mason J A, Veenstra M, Long J R. *Chem. Sci.*, **2014**,**5**:32-51

[3] Zhao M, Ou S, Wu C D. *Acc. Chem. Res.*, **2014**,**47**:1199-1207

[4] Cook T R, Zheng Y R, Stang P J. *Chem. Rev.*, **2013**,**113**:734-777

[5] Xuan W M, Zhu C F, Cui Y, et al. *Chem. Soc. Rev.*, **2012**, **41**:1677-1695

[6] Zhao D, Timmons D J, Yuan D Q, et al. *Acc. Chem. Res.*, **2011**,**44**:123-133

[7] Batten S R, Robson R. *Angew. Chem. Int. Ed.*, **1998**,**37**:1461-1494

[8] Batten S R. *CrystEngComm*, **2001**,**3**:67-72

[9] Carlucci L, Ciani G, Proserpio D M. *Coord. Chem. Rev.*, **2003**,**246**:247-289

[10]Wang X L, Qin C, Wang E B, et al. *Carlucci L. Angew. Chem. Int. Ed.*, **2005**,**44**:5824-5827

[11]Chen H Y, Xiao D R, He J H, et al. *CrystEngComm*, **2011**, **13**:4988-5000

[12]Yang Y, Du P, Liu Y Y, et al. *Cryst. Growth Des.*, **2013**,**13**: 4781-4795

[13]Yang J, Ma J F, Batten S R, et al. *Chem. Commun.*, **2008**: 2233-2234

[14]Wu H, Liu B, Yang J, et al. *CrystEngComm*, **2011**,**13**:3661-3664

[15]Cui Y F, Sun P P, Chen Q, et al. *CrystEngComm*, **2012**,**14**: 4161-4164

[16]Sun G M, Song Y M, Liu Y, et al. *CrystEngComm*, **2012**,**14**: 5714-5716

[17]Qin C, Wang X L, Wang E B, et al. *Inorg. Chem.*, **2008**,**47**: 5555-5557

[18]Ma Y, Ceng A L, Gao E Q. *Cryst. Growth Des.*, **2010**,**10**: 2832-2834

[19]Liu Y Y, Wang Z H, Yang J, et al. *CrystEngComm*, **2011**, **13**:3811-3821

[20]Gao J Z, Yang J, Liu Y Y, et al. *CrystEngComm*, **2012**,**14**: 8173-8175

[21]Hu F L, Wu W, Liang P, et al. *Cryst. Growth Des.*, **2013**,**13**: 5050-5061

[22]Blatov V A, Carlucci L, Ciani G, et al. *CrystEngComm*, **2004**,**6**:377-395

[23]Baburin I A, Blatov V A, Carlucci L, et al. *J. Solid State Chem.*, **2005**,**178**:2471-2493

[24]Guo H D, Qiu D F, Guo X M, et al. *CrystEngComm*, **2009**, **11**:2611-2614

[25]Liu F Q, Tilley T D. *Inorg. Chem.*, **1997**,**36**:5090-5096

[26]Cao T T, Peng Y Q, Liu T, et al. *CrystEngComm*, **2014**,**16**: 10658-10673

[27]Wang S N, Yun R R, Wang D Q, et al. *Cryst. Growth Des.*, **2012**,**12**:79-92

[28]Wang S N, Wang D Q, Dou J M, et al. *Acta Cryst. C*, **2010**, **66**:m141-m144

[29]Wang S N, Li D C, Dou J M, et al. *Acta Cryst. C*, **2010**,**66**: m118-m121

[30]Sheldrick G M. *SHELXS*-97, *Program for Crystal Structure Solution*, University of Göttingen, Germany, **1997**.

[31]Sheldrick G M. *SHELXL*-97, *Program for Refining Crystal Structure*, University of Göttingen, Germany, **1997**.

[32]Dolomanov O. *Olex Updated*. University of Nottingham, UK, **2005**.

[33]Kondo M, Yoshitomi T, Seki K, et al. *Angew. Chem. Int. Ed. Engl.*, **1997**,**36**:1725-1727

[34]Yaghi O M, Li H L. *J. Am. Chem. Soc.*, **1996**,**118**:295-296

[35]Power K N, Hennigar T L, Zaworotko M J. *New. J. Chem.*, **1998**,**22**:177-181

[36]Fu Z Y, Wu X T, Dai J C, et al. *New. J. Chem.*, **2002**,**26**: 978-980

[37]Ji C C, Li J, Li Y Z, et al. *CrystEngComm*, **2011**,**13**:459-466

[38]Spek A L. *J. Appl. Cryst.*, **2003**,**36**:7-13

[39]Li J R, Ma Y G, McCarthy M C, et al. *Coord. Chem. Rev.*, **2010**,**255**:1791-1823

[40]Zhang Y J, Liu T, Kanegawa S J, et al. *J. Am. Chem. Soc.*, **2010**,**132**:912-913

[41]Xiang H, Gao W Y, Zhong D C, et al. *CrystEngComm*, **2011**, **13**:5825-5832

[42]Chen M S, Chen M, Takamizawa S, et al. *Chem. Commun.*, **2011**,**47**:3787-3789